Interfacial potential approach for Ag/ZnO (0001) interfaces*

Song Hong-Quan(宋宏权)[a)c)†], Shen Jiang(申 江)[a)], Qian Ping(钱 萍)[a)], and Chen Nan-Xian(陈难先)[b)]

[a)] *Institute of Applied Physics, Beijing University of Science and Technology, Beijing* 100083, *China*

[b)] *Department of Physics, Tsinghua University, Beijing* 100084, *China*

[c)] *School of Physics and Mechanical & Electrical Engineering, Zhoukou Normal University, Zhoukou* 466001, *China*

(Received 4 May 2014; revised manuscript received 16 July 2014; published online 10 October 2014)

Systematic approaches are presented to extract the interfacial potentials from the *ab initio* adhesive energy of the interface system by using the Chen–Möbius inversion method. We focus on the interface structure of the metal (111)/ZnO (0001) in this work. The interfacial potentials of Ag–Zn and Ag–O are obtained. These potentials can be used to solve some problems about Ag/ZnO interfacial structure. Three metastable interfacial structures are investigated in order to check these potentials. Using the interfacial potentials we study the procedure of interface fracture in the Ag/ZnO (0001) interface and discuss the change of the energy, stress, and atomic structures in tensile process. The result indicates that the exact misfit dislocation reduces the total energy and softens the fracture process. Meanwhile, the formation and mobility of the vacancy near the interface are observed.

Keywords: zinc oxide, interfacial potential, inversion method, misfit dislocation

PACS: 68.35.–p, 68.55.–a, 68.35.Ct, 68.35.Ja **DOI:** 10.1088/1674-1056/23/12/126801

1. Introduction

ZnO is attracting intensive interest as being an important candidate for next-generation semiconductor electronics.[1] It has a direct and wide band gap of 3.4 eV. Therefore ZnO semiconductor can emit light in the near-UV spectral region at room temperature,[2,3] and has many advantages in optical and electrical properties. The transparent conducting oxide layers made by ZnO are suitable to be used as front electrodes in thin film solar cells.[4,5] The interface between the metal and zinc oxide plays a key role in various industrial applications such as catalysts, Schottky barrier diodes, and metal–oxide–semiconductor field-effect transistors.[6,7] And there are several reports for the metal/ZnO (0001) interface. For example, Jedrecy *et al.* studied the (Ag, Cu)/ZnO interfacial structures by X-ray measurements.[8–10] And Pt/ZnO is also widely investigated by X-ray and transmission electron microscope.[11–14] On the other hand, the theoretical works about metal/ZnO are mainly by the *ab initio* method.[15–19] But the molecular dynamics simulations are quite rare[20] because of the lack of interfacial potentials of metal/ZnO interface.

In this paper, our primary aim is to obtain the interfacial potentials suitable for metal/ZnO interface. In order to get those potentials, the Chen–Möbius inversion method was used.[21] This method assumes that adhesive energy of the interfacial structure is the sum of the pair interactions of the atoms across the interface. And then we can obtain the interfacial potentials of the atoms across the interface from the inversion formula. The Chen–Möbius method has been applied to many material systems such as ionic crystals,[22] semiconductors,[23] metal–rare earth compounds,[24] metal/MgO interfacial system,[25] metal/SiC interfacial system,[26–28] random allays system,[29] and metal/GaN interfacial system.[30] As a further application of Chen–Möbius inversion, we now investigate the metal/ZnO interfacial system. In this article, we focus on the study of the Ag/ZnO interfacial structure as an example.

The following work consists of three parts. In Section 2, we introduce the inversion formula for the Ag/ZnO (0001) interface. In Section 3, we extract the interfacial potentials from adhesive energies calculated by *ab initio* method. A series of checks show that the resultant potentials are self-consistent and also partially transferable. And then, using these potentials we simulate the fracture process of Ag/ZnO (0001) and discuss the results. This is the main purpose of the present work. Section 4 is the conclusion.

2. Methodology

2.1. Interface structures

There are Ag–Zn and Ag–O interfacial potentials, denoted as $\Phi_{\mathrm{Ag-Zn}}$ and $\Phi_{\mathrm{Ag-O}}$, cross the interface in the Ag/ZnO (0001) interfacial structure. We need to build two kinds of interface structures to obtain those potentials (see Fig. 1). *Ab initio* adhesive energies of two interface structures are used as the data source to derive interfacial potentials. Those two interface structures have the following characteristics for deriving a concise inversion formula. 1) Zn-terminated

*Project supported by the National Natural Science Foundation of China (Grant No. 50971024) and the National Key Basic Research Program of China (Grant No. 2011CB606401).

†Corresponding author. E-mail: shq.zknu@foxmail.com

© 2014 Chinese Physical Society and IOP Publishing Ltd

and O-terminated interface structures are taken into account. 2) The first layer of Ag is located on one-third of Zn–O bond. 3) The vertical distances between Zn and O are designed as 1:3.

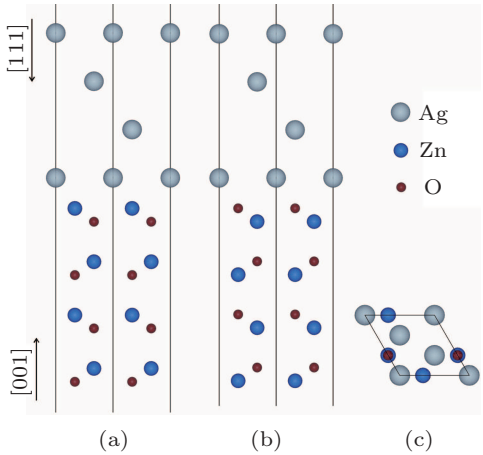


Fig. 1. (color online) Interface structures of Ag/ZnO (0001), (a) Zn-terminated, (b) O-terminated, and (c) top view of interface structures.

2.2. Inversion formula

In previous work, we have studied the Ag/GaN (0001) interface structure.[30] The inversion formula of Ag/ZnO is also the same because ZnO and GaN have the same crystal structure. So we briefly describe the process that is used for deriving the $\Phi_{\mathrm{Ag-Zn}}$ and $\Phi_{\mathrm{Ag-O}}$.

In a pair potential approach, adhesive energies of Zn-terminated interface structure and O-terminated interface structure, denoted as $E_{\mathrm{Zn-term}}$ and $E_{\mathrm{O-term}}$ respectively, are equal to the summation of $\Phi_{\mathrm{Ag-Zn}}$ and $\Phi_{\mathrm{Ag-O}}$, expressed as

$$E_{\mathrm{Zn-term}} = \sum_{r_a} a\Phi_{\mathrm{Ag-Zn}}(r_a(x)) + \sum_{r_b} b\Phi_{\mathrm{Ag-O}}(r_b(x)), \quad (1)$$

$$E_{\mathrm{O-term}} = \sum_{r_a} a\Phi_{\mathrm{Ag-O}}(r_a(x)) + \sum_{r_b} b\Phi_{\mathrm{Ag-Zn}}(r_b(x)), \quad (2)$$

where a and b are coordination numbers, r_a and r_b are interatomic distance across the interface.

For simplification, some intermediate variables are defined:

$$E_{\pm}(x) = E_{\mathrm{Zn-term}}(x) \pm E_{\mathrm{O-term}}(x), \quad (3)$$

$$\Phi_{\pm}(r) = \Phi_{\mathrm{Ag-Zn}}(r) \pm \Phi_{\mathrm{Ag-O}}(r), \quad (4)$$

then we can get

$$\begin{aligned} E_{\pm}(x) &= \sum_{r_a} a\Phi_{\pm}(r_a(x)) \pm \sum_{r_b} b\Phi_{\pm}(r_b(x)) \\ &= \sum_{p_{\pm}} p_{\pm}\Phi_{\pm}(r_{p_{\pm}}(x)), \end{aligned} \quad (5)$$

where $p_{\pm}$ is related with a, b, and $r_{p_{\pm}} \in \{r_a, r_b\}$.

Using the Chen–Möbius inverse method, we can obtain the interfacial potentials expressed as

$$\Phi_{\pm}(x) = \sum_{q_{\pm}} q_{\pm} E_{\pm}(r_{q_{\pm}}(x)), \quad (6)$$

where $q_{\pm}$ is inversion coefficient.

3. Results

3.1. Interfacial potentials

Now, we are in a position to get the pair potentials across the Ag/ZnO (0001) interface by using the pre-determined inversion formula. For this purpose, the *ab initio* calculation is performed with the generalized gradient approximation (GGA) by using the CASTEP code. The interactions between electrons and core ions are treated with an ultrasoft pseudopotential. The plane-wave cut-off energy is 450 eV and the k-point spacing is 0.03 Å^{-1}, which is generated by the Monkhorst–Pack scheme. And the energies on each atom are converged within 10^{-6} eV. Finally, $\Phi_{\mathrm{Ag-Zn}}$ and $\Phi_{\mathrm{Ag-O}}$ are plotted in Fig. 2(a) and they are fitted into the Rahman–Stillinger–Lemberg potential (RSL2) forms:

$$\begin{aligned} \Phi(R) = {} & D_0 \exp\left[y\left(1 - \frac{R}{R_0}\right)\right] + \frac{a_1}{1 + \mathrm{e}^{b_1(R-c_1)}} \\ & + \frac{a_2}{1 + \mathrm{e}^{b_2(R-c_2)}} + \frac{a_3}{1 + \mathrm{e}^{b_3(R-c_3)}}, \end{aligned} \quad (7)$$

the related parameters are listed in Table 1.

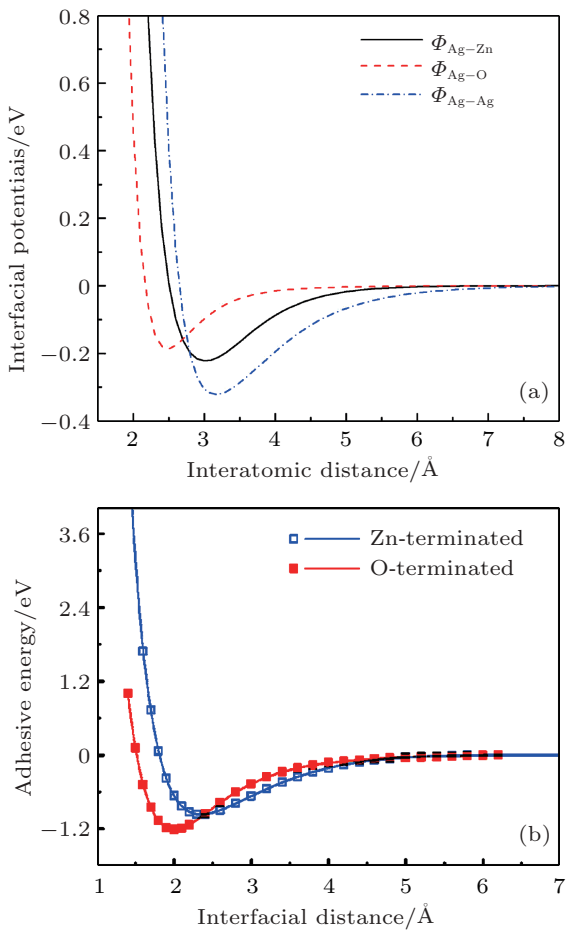


Fig. 2. (color online) (a) Potential curves of Ag/ZnO (0001) and $\Phi_{\mathrm{Ag-Ag}}$ for bulk Ag. (b) Comparison between the adhesive energies, obtained from an *ab initio* method and the inversed potentials, of the original structures used for inversion. The squares denote *ab initio* results, and lines denote the sum of inversed potentials.

Table 1. Potential parameters across the Ag/ZnO (0001) interface.

Atom pair	Potential parameters		
Ag–Zn	$D_0 = 4277.2935$ kcal·mol^{-1}	$R_0 = 1$ Å	$y = 4.2084$
	$a_1 = -0.5327$ kcal·mol^{-1}	$b_1 = 5.2619$ Å^{-1}	$c_1 = 3.5369$ Å
	$a_2 = -8.6798$ kcal·mol^{-1}	$b_2 = 1.8000$ Å^{-1}	$c_2 = 3.3262$ Å
	$a_3 = 0.0876$ kcal·mol^{-1}	$b_3 = 0.9656$ Å^{-1}	$c_3 = 0.6894$ Å
Ag–O	$D_0 = 3141.8234$ kcal·mol^{-1}	$R_0 = 1$ Å	$y = 5.0865$
	$a_1 = -35.2195$ kcal·mol^{-1}	$b_1 = 2.6489$ Å^{-1}	$c_1 = 2.1128$ Å
	$a_2 = 43.4220$ kcal·mol^{-1}	$b_2 = 2.6256$ Å^{-1}	$c_2 = 1.6708$ Å
	$a_3 = -9.1687$ kcal·mol^{-1}	$b_3 = 1.0508$ Å^{-1}	$c3 = 0.4472$ Å
Ag–Ag	$D_0 = 4760.9502$ kcal·mol^{-1}	$R_0 = 1$ Å	$y = 1.6171$
	$a_1 = -1747.8618$ kcal·mol^{-1}	$b_1 = 2.2129$ Å^{-1}	$c_1 = 1.6720$ Å
	$a_2 = -392.8310$ kcal·mol^{-1}	$b_2 = 1.4495$ Å^{-1}	$c_2 = 2.2826$ Å
	$a_3 = -13.0113$ kcal·mol^{-1}	$b_3 = 0.6884$ Å^{-1}	$c_3 = 0.0914$ Å

3.2. Testing of the pair potentials

It is worth paying attention to the validity and transferability of these potentials. In the first step, we recalculate the adhesive energies by the inversed potentials as shown in Fig. 2(b) as a self-consistent check. The result shows that the original *ab initio* adhesive energies can be precisely reproduced by the inversed potentials, and so it indicates that the inversion method is self-consistent. And then, we investigate the transferability from these interfacial potentials to some other interface structures. The corresponding interface structures are shown in Fig. 3(a)–3(f). Here we consider six different atomic configurations in three groups: (i) first-layer Ag on the T1 site, (ii) first-layer Ag on the T4 site, (iii) first-layer Ag on the H3 site. These interface structures and highly symmetrical sites (T1, T4, and H3) are shown in Fig. 3(g). For each case, both the Zn-terminated and O-terminated interfaces are taken into account.

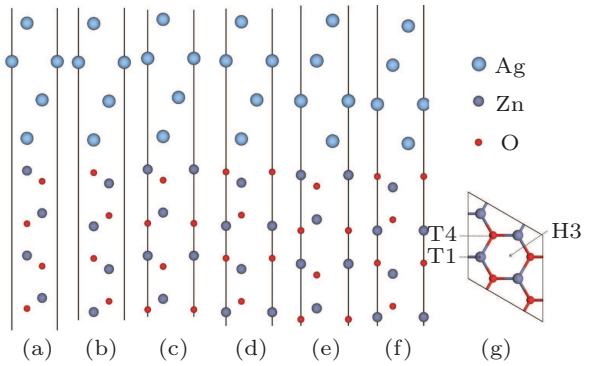


Fig. 3. (color online) Six interfacial models for additional checking. panels (a) and (b) are the T1-site structures, panels (c) and (d) are the T4-site structures, panels (e) and (f) are the H3-site structures. Among them, panels (a), (c), and (e) are Zn-terminated interfaces and panels (b), (d), and (f) are O-terminated interfaces. Panel (g) is atomic structures for the Zn-terminated of ZnO (0001) surface, showing high symmetry sites: T1-site, T4-site, and H3-site.

The resultant adhesive energies for these six models calculated by interfacial potentials and ab initio are presented in Fig. 4. The adhesive energies calculated by interfacial potentials are in good agreement with the result of ab initio for T4 site structures. However, it is in a poor precision for the O-terminated on T1 and H3 sites. Fortunately, it is good for the Zn-terminated on T1 and H3 sites. So these potentials are reasonable in describing the energy properties of Zn-terminated interface structures, because they can reproduce the *ab initio* adhesive energies for three highly symmetrical Zn-terminated interface structures. Therefore these potentials are limited to the calculation of Zn-terminated structures and not suitable for O-terminated structures. The main reason of this limitation is that O atoms are more electronegative and easier to form partially covalent bond. Therefore the potentials derived from O-terminated on T4 site are difficult enough to satisfy other sites.

3.3. Fracture process

Misfit dislocation plays a key role in determining the interfacial adhesion and fracture process. In many fracture experiments, the scale ranges from angstrom to millimeter. In this section, we investigate the fracture process of Ag/ZnO (0001) in the atomic scale. Dislocation must be considered on the fracture process because the surface mismatch magnitude of Ag/ZnO (0001) can reach as great as -11.1%.

3.3.1. Model

In order to acquire the clear images of fracture process and reduce the computational time, we pick a two-dimensional (2D) model as the research object. For the purpose of comparison, three kinds of interface model are built for Ag/ZnO (0001) interface fracture process, as shown in Fig. 5. Considering that ZnO lattice is much more rigid than Ag metal, we fix the atomic positions of Zn and O in the fracture process of those three models. In the first model, the metal slab is treated as a rigid body in the simulation in order to acquire a fundament understanding about the fracture process. This model is named as the rigid model and shown in Fig. 5(a). In the second model, seven layers of Ag have the characteristic of mobility.

This model is named coherent model as shown in Fig. 5(b). In the third model, the interfacial misfit dislocation is taken into account. We studied the atomic configuration of misfit dislocations in the Ag/ZnO (0001) in this section. It is mainly for the reason that the surface misfit dislocation of 11.1% leads to an almost perfect lattice coincidence every 9(8) Ag(ZnO) unit cells and this interface structure has been observed by some experiments. This model, named semicoherent model, is shown in Fig. 5(c).

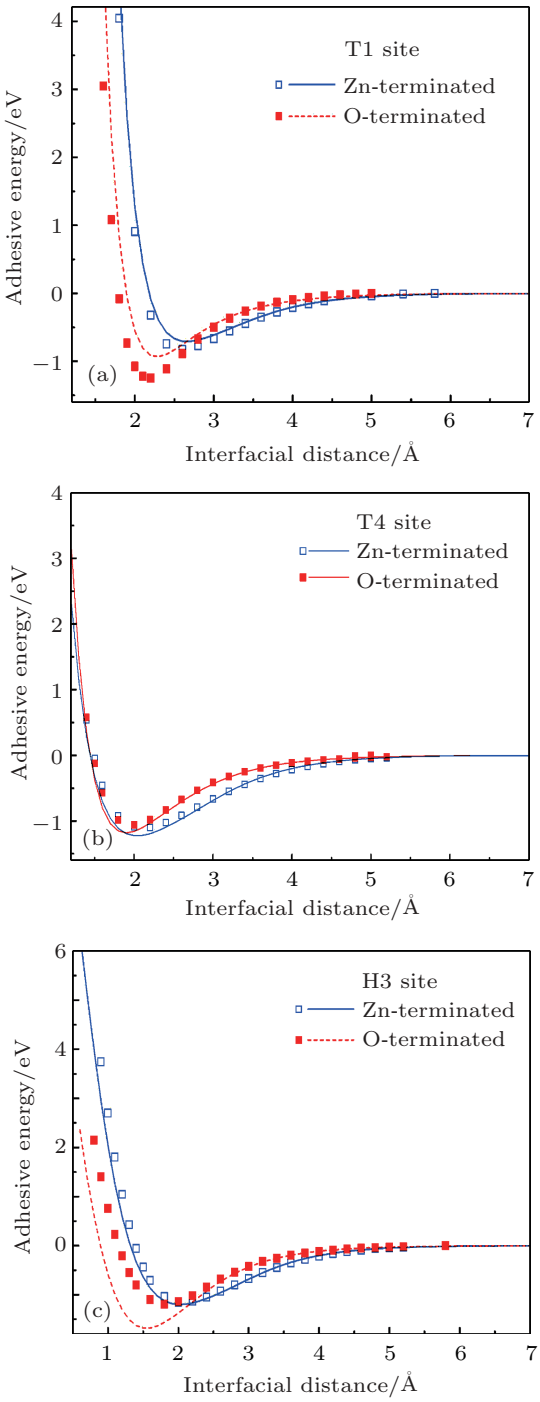


Fig. 4. (color online) Adhesive energy curves from *ab initio* calculation and summation of inversed potentials for Ag/ZnO (0001). Squares represent the *ab initio* results, and lines represent the summation of inversed potentials.

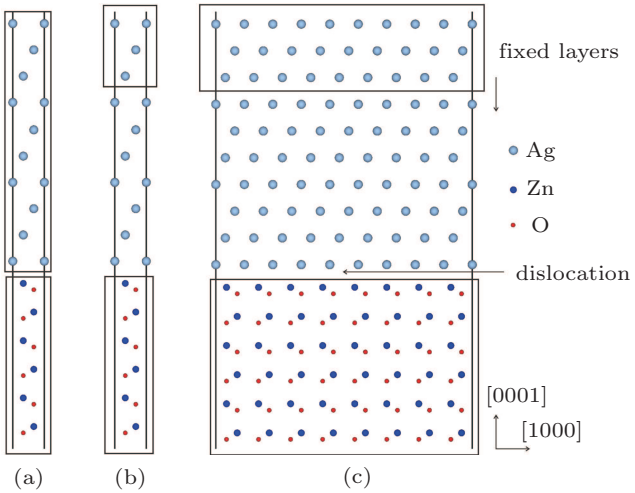


Fig. 5. (color online) The Zn-terminated models in the fracture process: (a) the rigid model, (b) the coherent model, and (c) the semi-coherent model.

In order to avoid the surface effects on the top and bottom of models, we choose ten layers of Ag and eight bilayers of ZnO. Those lengths are about 21 Å and 20 Å respectively, and they are enough to eliminate the surface effects.

3.3.2. Energy and stress

In the simulation, the fixed Ag layers are vertically moved by 0.01 Å. Then, the other atoms are relaxed by the energy minimization method. In the whole process, the resultant total energy per unit cell is shown in Fig. 6(a). The final energy at the end of the fracture process is defined as zero.

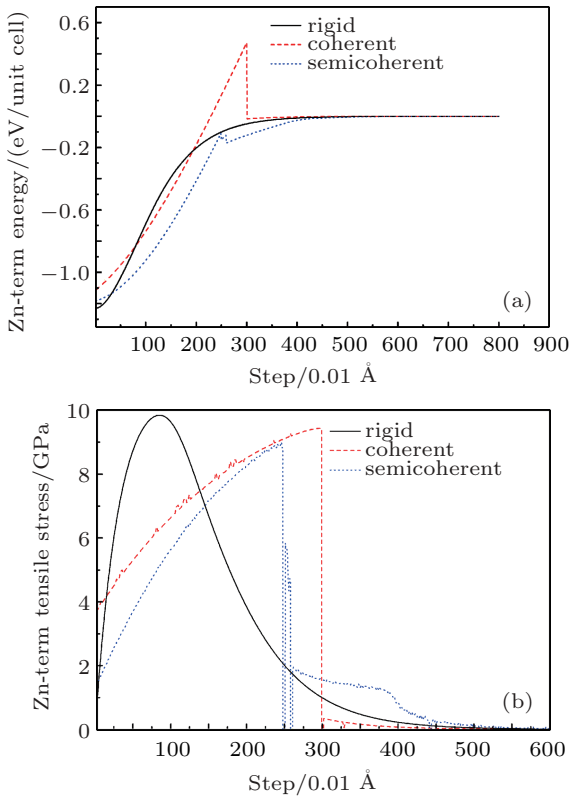


Fig. 6. (color online) (a) The energy of the three models in fracture process and (b) the tensile stress of the three models in fracture process.

We also calculate the tensile stress in the fracture process, using the formula

$$\sigma = \frac{1}{S}\frac{\mathrm{d}E}{\mathrm{d}x}, \tag{8}$$

where S is the interface area. Considering that the energy data are discrete and the interval of x is a constant (0.01 Å), the formula (8) can be expressed as

$$\sigma(n) = \frac{E_{n+1} - E_{n-1}}{2S\Delta x}, \tag{9}$$

the result of tensile stress is shown in Fig. 6(b). As can be seen from Fig. 6(b), the exact misfit dislocation reduces the total energy and softens the fracture process. In the whole fracture process of semi-coherent model, the change curve of tensile stress as a function of step has some jump points and can be divided by five stages. Corresponding atom structures are shown in Fig. 7.

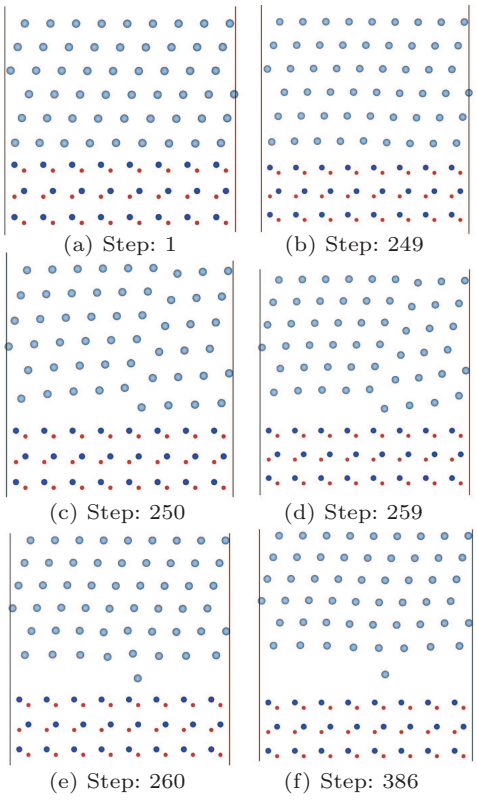


Fig. 7. (color online) The atomic structure change of Ag/ZnO (0001) in the fracture process.

We analyze every stage of tensile stress and corresponding atom structures, as presented below.

Stage 1 From step 1 to step 249, the tensile stress increases monotonously, while the slight change near the interface is observed. The distance between Ag atoms increases, while the dislocation core is still located on the interface.

Stage 2 From step 249 to step 250, a significant reduction of the tensile stress occurs, and a great change of atomic structure also takes place. Some vacant sites are formed on the interface near the dislocation core. During the deformation of the atomic structure, the strain energy is partly released.

Stage 3 From step 250 to step 259, the tensile stress is further reduced. Crack appears on part of the interface, and then expands rapidly.

Stage 4 From step 259 to step 260, the tensile stress decreases dramatically again and the interface is broken mostly. The arrangement of Ag atoms near the interface is similar to bulk, and only one Ag atom is still in contact with the ZnO.

Stage 5 From step 260 to step 386, the fracture is complete and one Ag atom sticks out the layers of Ag atoms in the end.

4. Conclusion

In this work, the Chen–Möbius inversion method is used to study the Ag/ZnO (0001) interface. The interfacial potentials are extracted from *ab initio* adhesive energies by using a concise and general inversion formula just based on the pairwise approximation. A series of additional *ab initio* calculations have been done for the purpose of checking the inversed potentials. And the results show that the resultant potentials are self-consistent and partially transferable. However, there are some limitations of this work besides those advantages. The inversed potentials are not totally transferable for an Ag/ZnO (0001) interface, but prefer the Zn-terminated interfacial system. Finally, we use those potentials to study the fracture process of Ag/ZnO (0001) by atomic simulation method. As a result, we have obtained the change of the energy, tensile stress, and atomic structure. With this result, we discovered that the fracture process of semi-coherent model can be divided into five stages. The misfit dislocation reduces the tensile stress and slows down the fracture process. Meanwhile, the interface nearby is easier to form vacancy because of the exact misfit dislocation. In summary, this method provides a way to obtain interfacial potentials from *ab initio* adhesive energies by using a universal formula suitable for Ag/ZnO (0001) or other interfaces within similar structures. Based on interfacial potentials, we can investigate many properties of the interface structure by the atomistic simulation.

Acknowledgments

The authors express their deep gratitude to Drs. Long Yao, Zhao Han-Yue and Li Jin-Chun for their interesting discussion and encouragement.

References

[1] Janotti A and van de Walle C G 2009 *Rep. Prog. Phys.* **72** 126501
[2] Thomas D G 1960 *J. Phys. Chem. Solids* **15** 86
[3] Reynolds D C, Look D C, Jogai B, Litton C W, Cantwell G and Harsch W C 1999 *Phys. Rev. B* **60** 2340

[4] Ramanathan K, Contreras M A, Perkins C L, Asher S, Hasoon F S, Keane J, Young D, Romero M, Metzger W, Noufi R, Ward J and Duda A 2003 *Prog. Photovoltaics* **11** 225
[5] Jia Z N, Zhang X D, Liu Y, Wang Y F, Fan J, Liu C C and Zhao Y 2014 *Chin. Phys. B* **23** 046106
[6] Klingshirn C 2007 *ChemPhysChem* **8** 782
[7] Qing J, Zhong Z F, Liu Y, Li B J and Zhou X 2014 *Chin. Phys. B* **23** 038802
[8] Jedrecy N, Renaud G, Lazzari R and Jupille J 2005 *Phys. Rev. B* **72** 045430
[9] Jedrecy N, Gallini S, Sauvage-Simkin M and Pinchaux R 2001 *Phys. Rev. B* **64** 085424
[10] Jedrecy N, Renaud G, Lazzari R and Jupille J 2005 *Phys. Rev. B* **72** 195404
[11] Blumentrit P, Yoshitake M, Nemsak S, Kim T and Nagata T 2011 *Appl. Surf. Sci.* **258** 780
[12] Murakami K, Saito M, Takuma E and Ichinose H 2003 *J. Electron Microsc.* **52** 27
[13] Nagata T, Volk J, Yamashita Y, Yoshikawa H, Haemori M, Hayakawa R, Yoshitake M, Ueda S, Kobayashi K and Chikyow T 2009 *Appl. Phys. Lett.* **94** 221904
[14] Saito M, Wagner T, Richter G and Ruhle M 2009 *Phys. Rev. B* **80** 134110
[15] Kamiya T, Tajima K, Nomura K, Yanagi H and Hosono H 2008 *Phys. Status Solidi A* **205** 1929
[16] Meyer B and Marx D 2004 *Phys. Rev. B* **69** 235420
[17] Northrup J E and Neugebauer J 2005 *Appl. Phys. Lett.* **87** 141914
[18] Yang Z and Xiong S J 2011 *Surf. Sci.* **605** 40
[19] Lin Z S and Bristowe P D 2007 *Phys. Rev. B* **75** 205423
[20] Cheng Y T, Liang T, Nie X W, Choudhary K, Phillpot S R, Asthagiri A and Sinnott S B 2014 *Surf. Sci.* **621** 109
[21] Chen N X 1990 *Phys. Rev. Lett.* **64** 1193
[22] Zhang S and Chen N X 2003 *Modelling and Simulation in Materials Science and Engineering* **11** 331
[23] Zhang S and Chen N X 2005 *Chem. Phys.* **309** 309
[24] Qian P, Su W, Shen J and Chen N X 2008 *Comput. Mater. Sci.* **43** 319
[25] Long Y, Chen N X and Wang H Y 2005 *J. Phys.: Condens. Matter* **17** 6149
[26] Wang Y D and Chen N X 2010 *J. Phys.: Condens. Matter* **22** 135009
[27] Zhao H Y, Chen N X and Long Y 2009 *J. Phys.: Condens. Matter* **21** 225002
[28] Zhao H Y and Chen N X 2008 *Inverse Probl.* **24** 035019
[29] Tian F Y, Chen N X, Delczeg L and Vitos L 2012 *Comput. Mater. Sci.* **63** 20
[30] Song H Q, Shen J, Qian P and Chen N X 2013 *Physica B* **431** 97